Thermoplastic Biodegradable Material Elaborated From Unripe Banana Flour Reinforced With Metallocene Catalyzed Polyethylene

E. San Martín Martínez,[1] M. A. Aguilar Méndez,[1] A. Sánchez Solís,[2] H. Vieyra[1]

[1] *Laboratorio de Biomateriales, Centro de Investigación en Ciencia Aplicada y Tecnología Avanzada del Instituto Politécnico Nacional, Colonia Irrigación, C.P. 11500, México, DF*

[2] *Departamento de Reología y Mecánica de Materiales, Instituto de Investigaciones en Materiales de la Universidad Nacional Autónoma de México, Ciudad Universitaria, Coyoacán 04510, México, DF*

To meet the challenge of procuring new sources of natural polymers without affecting the demands for food crops, a thermoplastic unripe banana flour (TPF) was produced, characterized, and blended with metallocene-catalyzed polyethylene (mPE). Both the pulp and peels of unripe banana were used to produce flour, whose stability and thermoplastic properties allowed blending with mPE in high proportions, that is, 50, 60, 70, and 80%. The blends were injection molded, and the thermal, mechanical, microstructural, and infrared spectral properties of the resulting samples were characterized. The blend containing 50% TPF yielded a robust, elastic, and nonbrittle material. Maleic anhydride grafting on mPE (mPE-*g*-MA) promoted interphase adhesion of the polymers and homogeneity in the blends. Grafting also influenced the mechanical, thermal, and microstructural properties of the blends. The characteristics of the blends make them ideal for designing biodegradable plastics while exploiting banana peels, which are usually considered agricultural waste. POLYM. ENG. SCI., 55:866–876, 2015. © 2014 Society of Plastics Engineers

INTRODUCTION

Starches from various sources (e.g., corn, potato, rice) are considered to be biodegradable components that can be employed in the plastics industry [1]. The structure and physicochemical properties of corn, rice, wheat, and potato starches have been well documented [2]. They can also be blended with synthetic polymers to improve their biodegradability properties [3, 4]. Nevertheless, because of the widespread use of starches, especially for food applications, new sources of these natural polymers that are appropriate for industrial purposes are required.

The complete unripe banana (peel and pulp) is of great interest as a candidate source of biodegradable materials. The unripe banana pulp contains up to 70–80% starch on a dry weight basis, a percentage comparable to that in the endosperm of corn grain and the pulp of white potatoes [5]. Furthermore, the banana peel, which is usually considered to be waste, can account for up to 40% of the total weight of a banana [6]. In general, plant cell wall polysaccharides are an extremely diverse set of biopolymers that play an important role as structural elements. They include both soluble fibers (pectins, gums, etc.) and insoluble fibers (cellulose, lignin, some hemicelluloses, etc.) [7]. Plant-derived fibers and crop derivatives of lignocellulosic composition have been reported to be good biodegradable reinforcing fillers [8–10]. Therefore, we hypothesized that the biopolymers of the banana peels might be useful as a filler and reinforcing material [11]. During banana ripening, the starch reserve rapidly transforms into sucrose and is further converted into glucose and fructose by the activities of amylase, glycosidase, phosphorylase, sucrose synthase, and invertase [12, 13]. Thus, for starch production, it is necessary to process the bananas while they are unripe.

Bananas are the fourth most important crop in the food industry worldwide, behind only rice, wheat, and corn [14]. Bananas grow throughout the year. Furthermore, unconsumed material is generally available [15], which is important because, as noted by other researchers, the low cost and availability of underutilized agricultural products make them suitable for the manufacture of new polymeric materials [16].

This study aimed to prepare unripe banana flour with potential for use as a matrix, not as a filler, for a biodegradable plastic material. Several granular starches have been blended with plastics to develop biodegradable materials [17]. However, the starch is often not well dispersed within the plastic matrix due to its inherent hydrogen bonding [18]. To avoid agglomeration and a lack of homogeneity in blending with synthetic polymers, thermoplastic starches (TPS) have been developed by incorporating appropriate amounts of water and/or plasticizers into the pristine starch [19]. Blends containing TPS have been shown to exhibit improved homogeneity compared to blends containing only native starch in their formulation, even when the same plastic matrix was used [20, 21]. Here, the thermoplasticization process was used to prepare unripe banana flour.

Polyethylene (PE) has the largest worldwide production volume of all synthetic polymers [22]. This polymer has many advantages, for example, low cost, excellent chemical resistance, lightness, durability, and lack of toxicity [23]. PE is synthesized using either Ziegler-Natta (ZN) catalysts or metallocene catalysts [24]. Ziegler–Natta catalysis produces a relatively broad distribution of molecular weights [25], and ZN-catalyzed PE products often have problems such as melt fracture, surface distortion, and deterioration of mechanical properties. Conversely, metallocene-catalyzed polyethylenes (mPEs) exhibit superior physical and mechanical properties because the metallocene

Correspondence to: Dr. Horacio Vieyra Ruiz; e-mail: horacio_vieyra_ruiz@yahoo.com.mx

Contract grant sponsor: The National Council of Sciences and Technology of Mexico (CONACYT); Contract grant sponsor: COFAA-IPN.

DOI 10.1002/pen.23954

Published online in Wiley Online Library (wileyonlinelibrary.com).

catalyst yields polyolefins with a narrow molecular-weight distribution and sparse long-chain branches [26]. Metallocene catalysis produces PE with an excellent degree of control over the molecular structure [27] and stereospecificity [28] at the commercial scale [29, 30]. In manufacturing, mPE is considered to be a good option among the available plastics because it has good mechanical properties.

A simple mixture of PE and starch lacks homogeneity [31] due to the nonpolar nature of PE. Grafting maleic anhydride to the backbone of the synthetic polymer can impart polarity to mPE [32]. Maleic anhydride increases compatibility and improves interphase adhesion between the natural and the synthetic polymer [33]. In this study, a thermoplastic unripe banana flour (TPF) was produced and characterized. The TPF was blended with mPE by extrusion, injection molded, and further characterized.

MATERIAL AND METHODS

Unripe Banana Flour

Unripe bananas (*Musa cavendishii AAA*) that had not been exposed to ethylene gas for ripening acceleration were purchased from Mexico City's supplies center. This type of banana is cultivated in the Gulf of Mexico and Ocean Pacific slopes (14°15′ and 22°30′ latitude north). Unripe bananas were sanitized with 1% sodium hypochlorite, cut longitudinally into 2 mm thick slices, and sprayed with 5% acetic acid to prevent enzymatic oxidation. The banana slices were dehydrated at 60°C for 36 h in a F.J. Stokes vacuum chamber (Philadelphia, USA), followed by powdering in a milling disc, sifting with a 40 mesh sieve, and re-sifting with a 100 mesh sieve to recover a fine-grained flour. The flour was subjected to a whitening process by mixing it with 40% hydrogen peroxide at a weight ratio of 6:4 in a Teledyne Lab internal mixer (York Pennsylvania) at a speed of 20 rpm for 60 min. This blend was dried for 24 h at 50°C, followed by an additional milling and sifting process. To generate thermoplastic material, the flour, water, and glycerol were mixed in the internal mixer at a 5:3:2 weight ratio for 30 min at 50 rpm. A fraction of the obtained material was dehydrated at 60°C for 36 h for characterization. The remaining material was reserved for blend preparation.

Functionalization of mPE

mPE Engage 8402 (Dow Chemical, Midland, MI), with a density 0.902 g/cm^3 (ASTM D 792) and melt flow index of 30 dg/min (190°C/2.16 Kg, ASTM D 1238), was mixed with 1% of maleic anhydride (99% purity from Sigma-Aldrich, St Louis, MO) and 1% of benzoyl peroxide (Luperox A75, 75% purity, Sigma-Aldrich) for 40 min. Maleic anhydride grafted mPE (mPE-*g*-MA) was extruded from a single-screw extruder (CICATA-IPN, Mexico City, Mexico; 60, 80,120, and 130°C in the heating zones and 45 rpm for the screw rotation) and then milled.

Preparation of TPF and mPE Blends

TPF, mPE, and mPE-*g*-MA were blended, extruded and injected using the following proportions: 50% TPF and 45% mPE (herein termed 50 TPF), 60% TPF and 35% mPE (herein termed 60 TPF), 70% TPF and 25% mPE (herein termed 70 TPF), 80% TPF and 15% mPE (herein termed 80 TPF), and 0% TPF and 100% mPE (herein termed neat mPE). All blends contained 5% mPE-*g*-MA.

Extrusion

TPF and the blends described above were extruded. Extrusion was performed at 80, 120, and 180°C in the three heating zones of the extruder and 200°C in the exit die. The mass flow and screw speed were set to 110 g/min and 30 rpm, respectively. A feeder (Baldor Electric, AR) was used to control the mass flow.

Colorimetric Analysis of the Flour

Five samples of the regular, unripe banana flour and the whitened flour were randomly selected for color index analysis. A Chroma Meter CR-400 (Minolta, Osaka, Japan) was employed. The color, represented as color difference ΔE^*, was calculated as:

$$\Delta E^* = [(\Delta L^*)^2 + (\Delta a^*)^2 + (\Delta b^*)^2]^{1/2} \quad (1)$$

where ΔL^*, Δa^*, and Δb^* are the differences between the color parameters of the samples and the white standard ($L^* = 93.49$, $a^* = -0.77$, $b^* = 1.40$) [34]. L^*, a^*, and b^* are parameters of the CIELAB system [35]. In this system, L^* represents lightness, and its value extends from 0 (black) to 100 (white); a^* Indicates the color ranging from red to green; and b^* indicates the color ranging from yellow to blue [36].

Viscosity Analysis

Samples consisting of 3.37 g of regular green banana flour and TPF (14% humidity) were supplemented with distilled water to reach a weight of 28.5 g before analysis in a Rapid Visco Analyzer (Newport Scientific, Australia). The following settings were used: 10 s for homogenization, followed by 5 min of heating from 50 to 90°C and 5 min at a constant temperature of 90°C. The samples were then cooled at 50°C for 6 min before analyzing their viscosity. The total elapsed time was 16 min at a constant speed of 160 rpm.

Measurement of Thermal Properties

Flour and injected samples were weighed and placed in hermetically sealed aluminum capsules. The samples were subjected to increasing temperature from 30 to 400°C at a rate of 10°C/min. Their melting temperature, gelatinization temperature, and enthalpy were determined in a Pyris 1, Perkin Elmer calorimeter (Norwalk, CT). Calibration was performed with indium, and an empty pan was used as the reference.

Injection Molding

Five samples of each blend and neat mPE were injected using a Demag Ergotech 50–200 system (Düsseldorf, Germany) with 50 tons of closing force. The samples were injected into an eight-cavity mold mechanical properties. The injection temperatures were 140, 150, 160, and 160°C for the heating zones, and the speed of the screw was 100 rpm. The injection mass flow rate was 30 cm^3/s, and the total volume for each injection was 75 cm^3. The cooling time between cycles was 20 s.

TABLE 1. Colorimetric analysis of regular and whitened unripe banana flour.

	Regular flour				Whitened flour			
Sample	L^*	a^*	b^*	ΔE^*	L^*	a^*	b^*	ΔE^*
1	14.38	0.53	3.13	79.14	27.5	−0.77	5.32	66.07
2	15.11	0.44	3.17	78.41	27.9	−0.7	5.51	65.73
3	14.66	0.43	3.14	78.86	28.8	−0.73	5.57	64.81
4	14.46	0.47	3.16	79.06	28.3	−0.68	5.52	65.33
5	14.65	0.44	3.15	78.87	27.3	−0.51	5.32	66.32
Mean	14.65	0.46	3.15	78.87	27.96	−0.68	5.45	65.65
Standard deviation	0.28	0.04	0.02	0.28	0.60	0.10	0.12	0.60

Mechanical Properties

The standard test method ASTM D638-10 for measuring the tensile properties of plastics was used to characterize the injected samples. All samples were conditioned for 96 h at 23°C and 50% relative humidity in accordance with ASTM D618-08 prior to testing. Five specimens for each sample (in the form of standard dumbbell-shaped test specimens) were used to test tensile resistance and elongation. Testing was performed on an Instron instrument (model 5583, MA), having a load capacity of 150 kN and a weight capacity of 500 kg. A testing speed of 50 mm/min was used. The results were analyzed using the mechanical testing software Bluehill 3.11 (Illinois).

Microstructural Analysis

Samples of unripe banana flour, TPF, and injected specimens were mounted on brass stubs with double-sided graphite-filled tape and were vacuum coated with silver by sputtering (Desk IV, Denton Vacuum). SEM micrographs were obtained at magnifications of 100×, 250×, 500×, 1000×, and 1500× (JSM-6390LV, JEOL, Japan).

Fourier Transform Infrared Spectroscopy (FT-IR) Analysis

FT-IR spectra of banana flour, TPF, neat mPE and injected samples of each blend were obtained using an Attenuated Total Reflectance FT-IR spectrophotometer (Spectrum Two, Perkin Elmer, MA). The wavelength range analyzed was 500–4000 cm^{-1}. The samples were pressed against the objective lens and analyzed directly.

Composting

Thermoplastic flour and metallocene catalyzed PE injection molded blend samples (80/20, 70/30, 60/40, 50/50, and 0/100, TPF/mPE, respectively) were fixed in a 15 × 20 cm^2 plastic grid. Five plastic grids were prepared (one for each time point). The grids were buried between two layers of Organodel compost (Agroformuladora Delta, Mexico), a lower layer of 60 cm and an upper layer of 30 cm. To facilitate further localization, the plastic grids were placed according to the time at which they would be collected, and a labeled flag was used to indicate their locations. After 25, 50, 75, 100, and 125 days under the compost, the grids were removed.

Weight Loss

Samples were retrieved from the grids and washed with deionized water. Retrieved specimens were dried for 24 h at 50°C and allowed to sit for 12 h at room temperature. All samples were weighed using an analytical balance, and the percentage of weight loss was calculated as follows:

$$\text{Weight loss}(\%) = \frac{\text{Initial weight} - \text{Final weight}}{\text{Initial weight}} \times 100 \quad (2)$$

SEM Analysis after Composting

The samples were chronologically observed at 0 days (as a control) and at 25, 50, 75, 100, and 125 days under compost. SEM (5 × 5 mm^2) coupons obtained from the samples were mounted on brass stubs with double-sided graphite-filled tape and were vacuum coated with silver by sputtering (Desk IV, Denton Vacuum). SEM micrographs were obtained at magnifications of 500×, 1000×, and 1500× (JSM-6390LV, JEOL, Japan).

RESULTS AND DISCUSSION

Colorimetric Analysis

Because the color of the final product is a critical quality parameter for acceptance by consumers, measuring the color of unripe banana flour is relevant for industrial decision making [37]. Unlike starch from corn, rice, and potatoes, the color of our unripe banana flour is brownish. Table 1 shows the color measurements of the flour. Taking into account the CIELAB parameters of the white standard, the mean L^* value of 14.65 ± 0.28 correlated with the low lightness of the flour. The high a^* value of 0.46 ± 0.04 indicated that the material was more red in color. The average b^* value of 3.15 ± 0.2 (deeper yellow) also correlated with the brownish color of the flour. In addition, the large ΔE value observed (78.87 ± 0.28) is consistent with the lack of whiteness in our flour [38]. The ΔE value indicates the numerical difference between white and the flour color [39]. Similar to regular starch, it is possible to apply either a bleaching treatment or a coloring process in a blend with a synthetic polymer. The whitening process resulted in an improvement of the color parameters L^* (27.96 ± 0.6), a^*(-0.68 ± 0.1), and b^* (5.45 ± 0.12), as well as the color difference ΔE (65.65 ± 0.6) of the flour compared with the white standard. The whitened flour acquired an acceptable yellowish color rather than the original brownish color.

Although the raw material was sprayed with a 5% acetic acid solution to prevent oxidation, the fact that the fruit is highly susceptible to enzymatic browning may explain the color of the flour. This browning process occurs because cutting or peeling the fruit exposes enzymes, such as polyphenol oxidase, to oxygen [40]. The brownish color of the flour could also be

 DOI 10.1002/pen

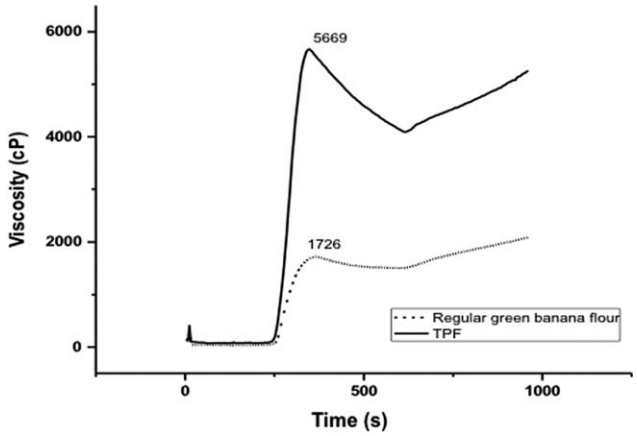

FIG. 1. Viscosity of the regular and the thermoplastic green banana flour.

attributed to the fibrous component of the flour, the banana peel. In terms of color appearance, the flour may be of interest for blending with polyolefins to create recycled and biodegradable products, as appearance is not the most important attribute of these materials.

Viscosity Analysis

Because our flour is composed mostly of starch, its capacity to form a viscous paste or a gel was determined by viscosity analysis after a heating and cooling process. A difference was observed between the maximum viscosity peaks of the regular flour and the TPF (1726 and 5669, respectively; Fig. 1). This difference of 3493 centipoises (cP) indicated that the glycerol added to the flour for thermoplasticization could be acting as a coating that prevents water from permeating into the starch granules. This effect would reduce the amount of swelling, which leads to granular breakage and determines the viscosity. Despite the difference, both samples had the ability to form gels.

The viscosity of both our flour preparations differed from the viscosity of the normal banana starch, which had a viscosity maximum peak of 2880 cP, as previously reported by others [41, 42]. It is remarkable that the addition of glycerol contributed to a two-fold change in the viscosity of the TPF. This large difference in viscosity may be due to the interaction of the amylose and amylopectin components of the starch with glycerol. The hydroxyl groups of starch form hydrogen bonds with those of glycerol, reinforcing the structure of the blend. This behavior would decrease the hydration of the material by neutralizing the hydration sites and, therefore, produce a viscous fluid whose viscosity would correlate with the amount of glycerol in the formulation [43, 44]. The rather small amount of cellulose fibers from the banana peels may have little influence in viscosity. Because temperature, humidity, and velocity are involved in the analysis, this characterization is useful for predicting the rheological behavior of TPF in the extrusion process.

DSC Analysis

In polymers, DSC can reveal thermal transitions, such as the melting temperature (T_m), crystallization temperature (T_c), and glass transition temperature (T_g) [45]. Gelatinization is a very important phase transition and is used to describe the molecular behavior of starch and relate it to the heat and moisture content [46]. DSC analysis also indicates the amount of energy, more specifically, the enthalpy, required for a state transition.

When analyzing the whole meal banana flour, well-defined peaks (endothermic events in the DSC curves) occurring between 165 and 170°C (Fig. 2a) were observed. These peaks

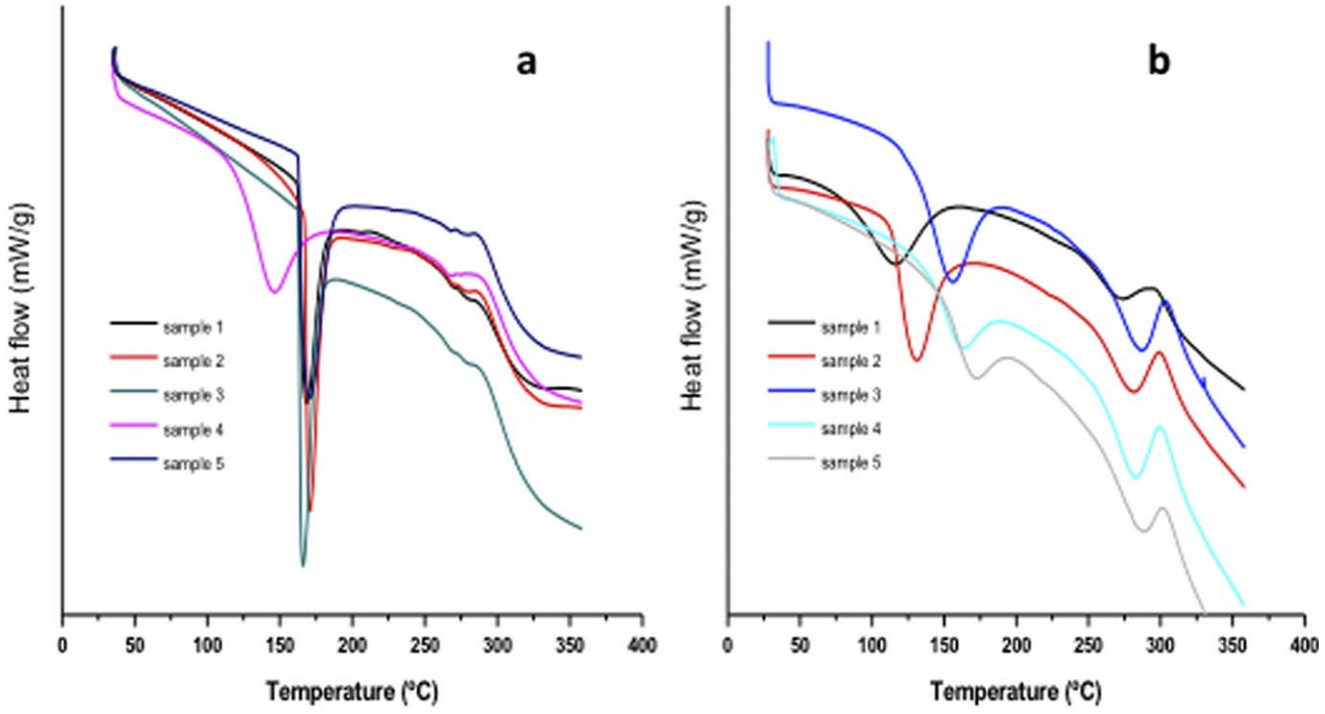

FIG. 2. Differential scanning calorimetry for regular (a) and thermoplastic (b) unripe banana flour. [Color figure can be viewed in the online issue, which is available at wileyonlinelibrary.com.]

TABLE 2. Melting temperatures (T_m) and Enthalpy (ΔH) for regular and TPF.

	Regular flour		TPF			
	Endothermic peak		Endothermic peak		Endothermic peak	
Sample	T_m (°C)	ΔH (J/g)	T_m (°C)	ΔH (J/g)	T_m (°C)	ΔH (J/g)
1	168	220	130	157	299	46
2	170	172	155	127	303	62
3	165	220	161	57	300	72
4	170	221	170	71	302	23
5	161	185	115	199	296	38
Mean	166.8	203.6	146.2	122.2	300	48.2
Standard deviation	3.8	23.4	22.9	59.2	2.7	19.4

were attributed to the melting temperature of the flour. Banana starch gelatinization has been reported to produce a peak between 70 and 74.5°C and an enthalpy value of 17.5 J/g [47]. Considering that banana flour can have a starch content as high as 80%, the inability of the flour to reach gelatinization at the same temperature as the starch, as well as the difference in the enthalpy value, may be the result of the humidity difference. Other constituents of the banana peel, such as cellulose, hemicelluloses, lignin, and others, could also modify the temperature and the energy required for fusion [48]. The enthalpy of the regular flour (Table 2) was higher than that reported for common starch [49].

The thermal transitions of the thermoplastic flour were markedly different. The thermograms appeared to be affected by the glycerol and endothermic transformations. Figure 2b shows two peaks. The first peak occurred between 115 and 170°C, which was slightly lower than that of the regular flour but higher than that reported for common starch, and the second peak occurred at 300°C. The enthalpy was also lower than that of the regular flour but higher than that expected for common starch (Table 2). Thermoplasticization may have influenced the thermal stability of the flour, and the exothermic peaks that appeared at 300°C, which were barely detectable in the regular flour, could be attributed to the thermal degradation of the cellulose [50, 51]. Because the flour could be used as the base for a biodegradable material manufactured by extrusion and injection molding, these results could be advantageous, as an excess of humidity would make the extrusion process difficult. In addition, analysis of the melting temperatures provided a basis for the extrusion differential heating program.

Further, the blends of TPF and mPE were analyzed. Figure 3 shows a comparative analysis of the two main components, the grafting reactant, and the blends. Neat mPE has been reported to have a melting peak at 65°C [52], and our result from the neat mPE thermo scan was 67°C. The scans of the blends were slightly shifted to the right, and increases in the flour concentration reduced the intensity of mPE melting peak. The TPF yielded two peaks at ~150 and 300°C, as previously observed. Maleic anhydride showed three very well defined peaks. The last two MA melting peaks (~230–260°C), the second flour peak and the neat mPE seemed to interact to yield a singular thermal behavior in the range of 250–320°C that appeared for all the blends. For that reason, the peculiar thermograms of the blends were assumed to be the result of the grafting process, as well as the presence of cellulose and the additional constituents of the flour (pectins, gums, lignin, and the glycerol added for thermoplasticization), which would require extra energy for their melting. In a previous thermal stability study, it was reported that the degradation of mPE and corn starch blends initiates at 320°C [1]. This information is important to graphically confirm the thermal degradation of the blend material in the 250–320°C interval. Thermal degradation at this temperature range was also observed after completing the calorimetric study, when the pans were opened.

Mechanical Properties

The mechanical properties of biodegradable materials determine their primary applications. Biodegradable materials prepared from synthetic polymer-starch blends and those derived from renewable organic sources commonly possess diminished mechanical properties, such as tensile resistance, compression resistance, and elongation, compared with regular plastics [53]. Thus, it is necessary to improve the mechanical properties of materials that are designed to be biodegradable plastics.

To assess the effectiveness of our polymer blends, the mechanical properties of injected neat mPE as well as the blends were evaluated. Figure 4a shows a difference of 0.153 MPa (11.71%) in the tensile strength at break between neat mPE mean and 50 TPF. For biodegradable materials design, the difference in tensile strength between neat mPE and 50 TPF is promising, considering the amount of flour used in its preparation. Unexpectedly, the tensile strength of 60 TPF was greater than that of neat mPE, which was a positive result considering its TPF content. The tensile resistance at break of the 80 and 70

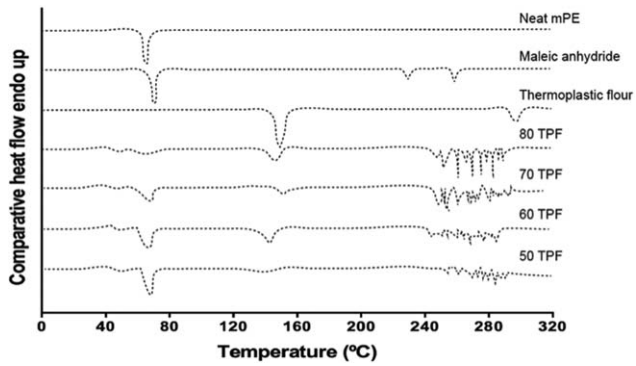

FIG. 3. Differential scanning calorimetry. Depicted are the thermograms of the neat components and the injected blends.

DOI 10.1002/pen

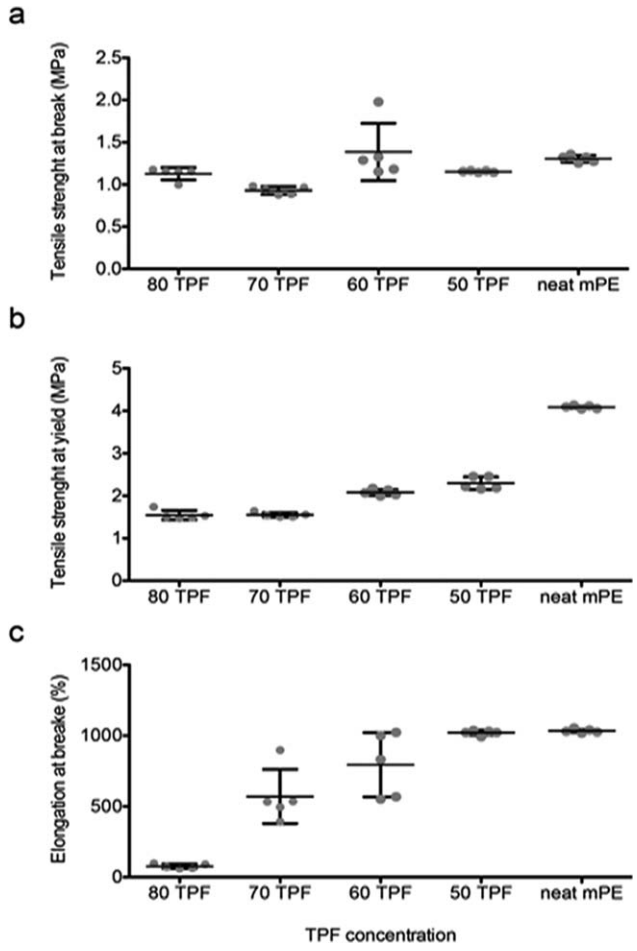

FIG. 4. Mechanical properties of the injected blends and injected neat mPE. (a) Tensile strength at break. (b) Tensile strength at yield, and (c) Elongation at break.

TPF blends was slightly lower, and the difference only reached 0.377 MPa (28.86%) compared with neat mPE. Lower values of tensile resistance were expected for these two last concentrations because of their larger content of flour.

The tensile resistance at yield, which is the maximum load that a given material resists, was also evaluated. As expected, neat mPE had the best tensile resistance, 4.0 MPa. However, the mean of 2.296 MPa for 50 TPF is a notable result for a natural-synthetic polymer blend, especially considering that this tensile resistance value indicated an average load resistance of 95.53 N. The tensile resistance at yield decreased when the percentage of TPF was increased in the blend.

It has been reported that the addition of a natural polymer such as starch or flour to a synthetic polymer generally results in decreased elongation at break [54]. This decrease is due to the immiscibility between the two components. The addition of maleic anhydride, thermoplasticization of the unripe banana flour, and the homogenization process minimized the immiscibility of our blends. Neat mPE and 50 TPF (Fig. 4c) had practically the same elongation at break. Chemical interactions between the biopolymers from the flour, glycerol, and mPE-*g*-MA generated a compact polymeric matrix, which could have helped to improve the elongation at break. When the flour content increased, the elongation capacity of the material decreased. The results remained good for 60 and 70 TPF (794.69 and 570.79%, respectively). However, the elongation at break for 80 TPF was not sufficient to consider that blend adequate for further utilization.

Microstructure Characteristics

The morphology and size of starch granules depend on the source plant [55]. Starch granules range between 1 and 110 μm. The granules of our unripe banana flour (Fig. 5a and b) averaged 30 μm, which is similar to granules from potato starch [56] and larger than the granules of rice and corn starch. SEM micrographs showed ovular and irregular granules, as well as amorphous structures consistent with insoluble fibers. Although the proportion of fibers observed was low, DSC measurements revealed that fibers exert an influence on the thermal properties of the flour by raising the fusion temperature of the banana starch [57, 58]. In addition, the thermoplasticization process did not have a detrimental effect on the morphology and microstructure of the unripe banana flour (Fig. 5c and d).

The behavior of the starch and the flour, when subjected to high temperatures, has been reported to depend on the moisture level [2, 59]. Extrusion of the regular banana flour, which was performed in humidified conditions, produced a homogeneous

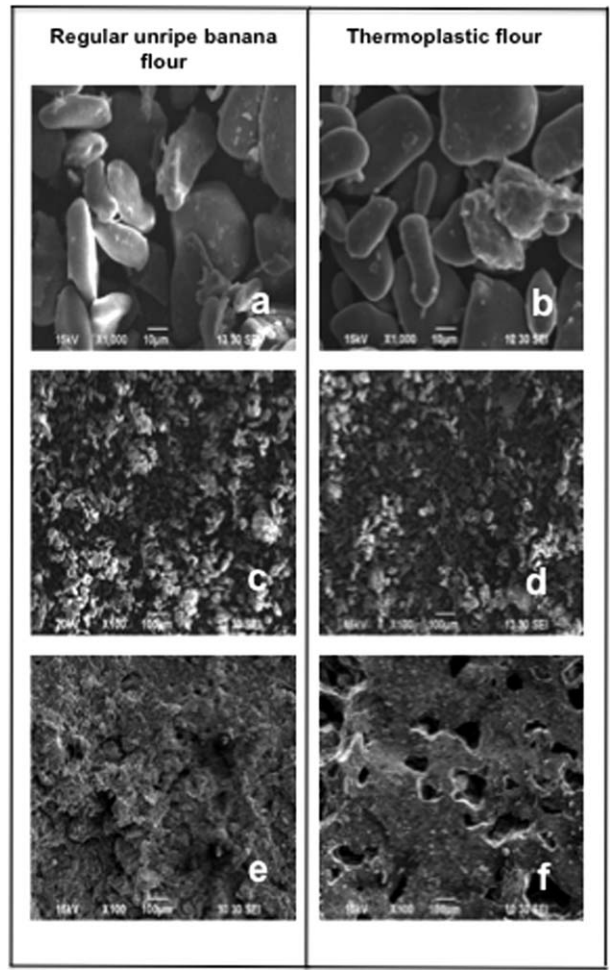

FIG. 5. Scanning electron microscopy of regular and TPF: (a,b) granule size and shape, (c,d) distribution of flour particles, and (e,f) microstructure of extruded flour.

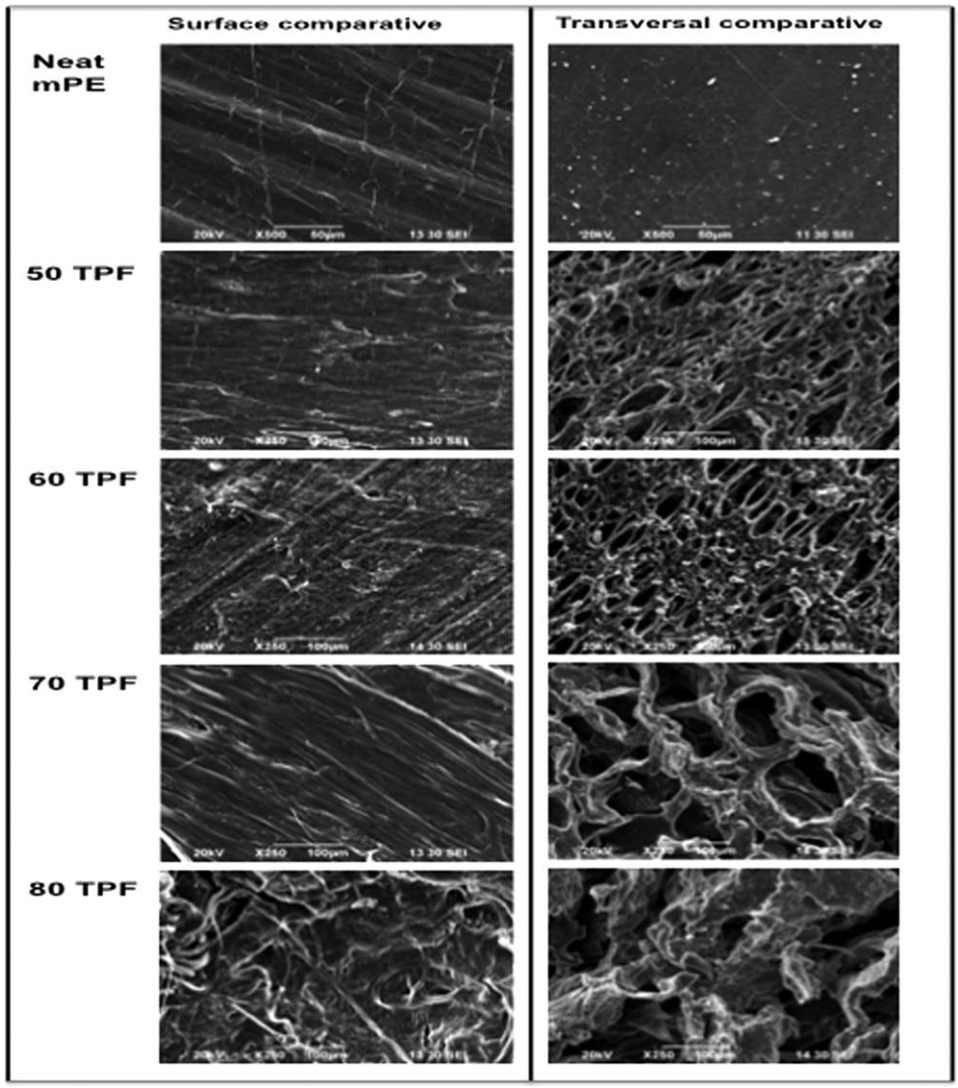

FIG. 6. Scanning electron microscopy of the mold injected material. Surface and transversal view of the different TPF preparations.

material (Fig. 5e). Extrusion of the thermoplastic flour, which was performed in dry conditions, produced a porous material (Fig. 5f). The pores were most likely generated because, in absence of humidity, glycerol prevents the gelatinization of the starch granules, generating a noncompact structure. Moreover, the resultant extruded material was rigid, hard and frail. In contrast, when the banana flour was humidified before extrusion (Fig. 5e), the heat caused the water to flow through the starch granules, thereby improving gelatinization and further plasticization. Thus, the extruded flour was compact and fibers appeared to be integrated.

Because microstructural analysis is important for explaining the mechanical properties, SEM analysis of the injected blends was performed, both at the surface and in the transverse plane. For neat mPE, the direction of the flux of injected material was evident. These samples presented a practically a smooth surface with no discontinuities or cavities that could affect the mechanical properties, and the transverse view revealed a uniform texture (Fig. 6). The 50 TPF blend exhibited a slightly rough surface, and the injection flux appeared somewhat discontinuous, though the direction was well defined; the transversal view revealed a porous structure that could be explained by the glycerol content and insufficient humidity level, which prevented the gelatinization of the starch granules. The porosity at this flour concentration most likely contributed to the characteristics of the final material, which was robust, elastic, and nonbrittle. A similar study found that morphological characteristics were drastically affected by polymers containing anhydride functional groups, such as mPE-*g*-MA [60].

More irregularities were visible on the 60 TPF surface. Although no major visual differences existed between 50 and 60 TPF (transverse view), their mechanical properties differed in a TPF-mPE ratio-dependent manner. The surface of 70 TPF showed a uniformly oriented fibrous structure, and the transverse view showed a honeycomb pattern, which most likely originated from the greater proportion of starch and cellulose fibers from the unripe banana flour as well as the humidity level. The 80 TPF was disorganized, had cavities and discontinuities, and no layer formation was observed. This microstructure may explain its poor mechanical properties.

 DOI 10.1002/pen

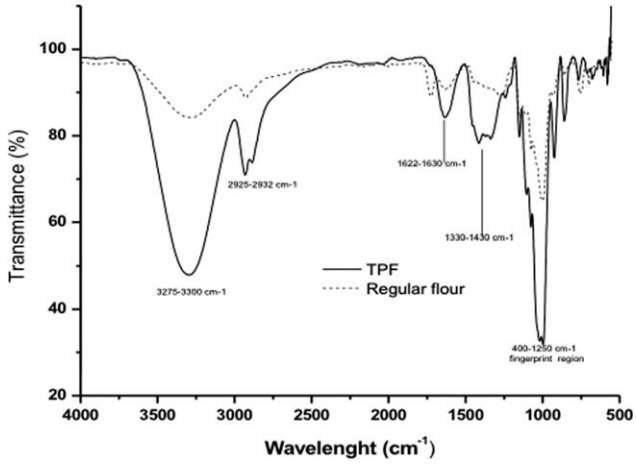

FIG. 7. Fourier-transformed infrared spectroscopy (FT-IR) analysis for regular green banana flour and TPF.

It is worth mentioning that, even at the higher flour proportion, starch cumulus never appeared. This result suggests not only a physical or heterogeneous blending but also interaction between the starch, cellulose, and mPE induced by the maleic anhydride. Both superficial and transverse micrographs elucidate that the mechanical properties observed for our blends depended on the level of porosity, the size of the cavities, the absence of a pattern and the disoriented microstructure. Microstructural changes were correlated with reductions in the tensile resistance and elongation.

FT-IR Analysis

FT-IR spectra of the regular and TPF were obtained (Fig. 7). The spectra of both materials were similar. A peak between 3275 and 3300 cm^{-1} that is characteristic of the stretching vibration of the hydroxyl group (—OH) in cellulose and starch [61] was observed. The spectrum of the TPF showed an increase in the width of this peak because the three —OH groups of the glycerol [$C_3H_5(OH)_3$] contributed to the peak intensity. The peak at 2925–2932 cm^{-1} was attributed to the vibration of the asymmetric tension of the —CH_2 group [62]. The peak between 1622 and 1630 cm^{-1} corresponded to linked water absorption. The crest at 1330–1430 cm^{-1} was associated with the bending vibration of the —OH group. Three peaks appeared in the fingerprint region from 400 to 1250 cm^{-1}, which are common in the banana starch. The first one (923–1150 cm^{-1}) and the second one (1148–1150 cm^{-1}) were attributed to the C—O stretching vibration mode [63], and the third peak is characteristic of the C—O—C groups in glycosidic units or the β-(1–4) glycosidic linkages between glucoses in cellulose (1160 cm^{-1}). The band observed at 860 cm^{-1} corresponded to the harmonic vibration of C—H in starch [64] and was larger in TPF.

When analyzing the blends of TPF and mPE, a similar pattern that resembled the TPF spectrum with the incorporation of PE characteristics was observed for all blends (Fig. 8). The peaks characteristic of TPF were the broad absorption band of the stretching vibration of the hydroxyl groups (—OH) in cellulose, starch, and glycerol (3307–3292 cm^{-1}); the hemiacetal bonds from the starch flour (1638–1650 cm^{-1}); the vibration peak corresponding to the cyclic —C—C— of the glucose (1030–1018 cm^{-1}) in the starch; and the 1151, 924, and 860 cm^{-1} peaks corresponding to the fingerprint region of the banana starch. The mPE in the blends contributed additional peaks to the spectra: the symmetric and asymmetric (2918 and 2850 cm^{-1}) stretching bond vibrations of the —CH_2 and CH_3 groups in mPE [25]; the characteristic —CH_2 stretching for the oxidation of synthetic polymers (1460 cm^{-1}); the angular deformation absorption group CH_3 (1375 cm^{-1}) and the 719 cm^{-1} band, which is typical of PE, also appeared.

The mPE-*g*-MA spectrum was included, and the absorption peaks of the anhydride group (1791 and 1714 cm^{-1}) were circled to highlight them. The MA carbonyl stretching absorption band at 1791 cm^{-1} indicated that a specific quantity of MA group was grafted onto the molecular chains of mPE. Another carbonyl symmetric stretching absorption band at 1714 cm^{-1} was expressed and confirmed the presence of MA. Although these MA peaks were not visible in the spectra of the blends (mPE, banana starch and mPE-*g*-MA), the homogeneity of the blends, demonstrated by their mechanical, thermal, and microstructural properties, can be attributed to the interphase adhesion promoted by MA grafting.

Weight Loss

Weight loss is one of the indicators of biodegradation [65]. Figure 9 shows the results of weight loss monitoring for the samples during composting. The control sample (neat mPE, 0 TPF) had the smallest weight loss after 125 days. The minimal effect of composting on the mPE was most likely due to its natural resistance to microbial attack [66]. The lowest weight loss of all the blends was observed for 50 TPF. Perhaps the homogeneity of this blend, resulting from the functionalization of the mPE, allowed it to resist the enzymatic action of microorganisms due to increased polymer-flour interfacial adhesion. Thermogravimetric assays have previously reported a decrease in the degradation rate due to MA grafting [67]. The blends 60, 70, and 80 TPF lost a considerable amount of weight. The 70 TPF lost 40% of its weight in a short time, but the 80 TPF lost half of its weight as early as 50 days under compost. The thickness of the samples was 4 mm. Thus, the observed weight loss rates

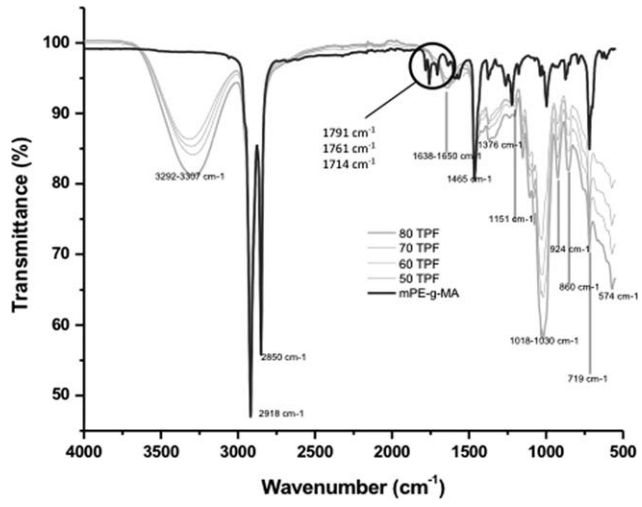

FIG. 8. FT-IR spectra of the blends from 50 to 80 TPF and mPE-*g*-MA. Circle encloses the three peaks from MA.

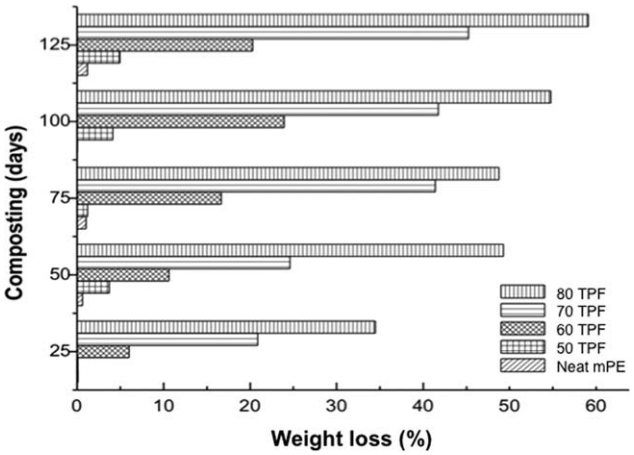

FIG. 9. Relative weight loss percentage data at 25 days intervals.

revealed a good tendency of deterioration. Interestingly, all the samples, including the neat mPE, lost more than half of their final weight loss value in the first 50 days. The results suggested that higher flour content increased susceptibility to microbial enzymatic attack, consequently improving biodegradation [68].

SEM Microstructural Analysis

Biodegradation under compost begins with an erosion process [69], caused by microorganisms and the environment. Indicators of erosion include fractures, breaches, cavities, and holes. All these indicators can be monitored by scanning electron microscopy. SEM analysis allows a visual tracing of biodegradation when material has undergone composting [70].

The changes in the microstructure of all samples subjected to composting in this study (Fig. 10) were monitored. The neat mPE sample showed a smooth surface that remained practically intact in the micrographs from 0 to 100 days. Only the final observation at 125 days exhibited slight deterioration, indicated by very small pores. This observation correlates with the weight loss measured for this sample. All TPF/mPE blends underwent intense changes during composting. The 50 TPF sample showed a semi-flat surface, and the flux of the injection could only be perceived at day 0. However, deterioration within 100 days caused some breaches and holes, and deterioration was even

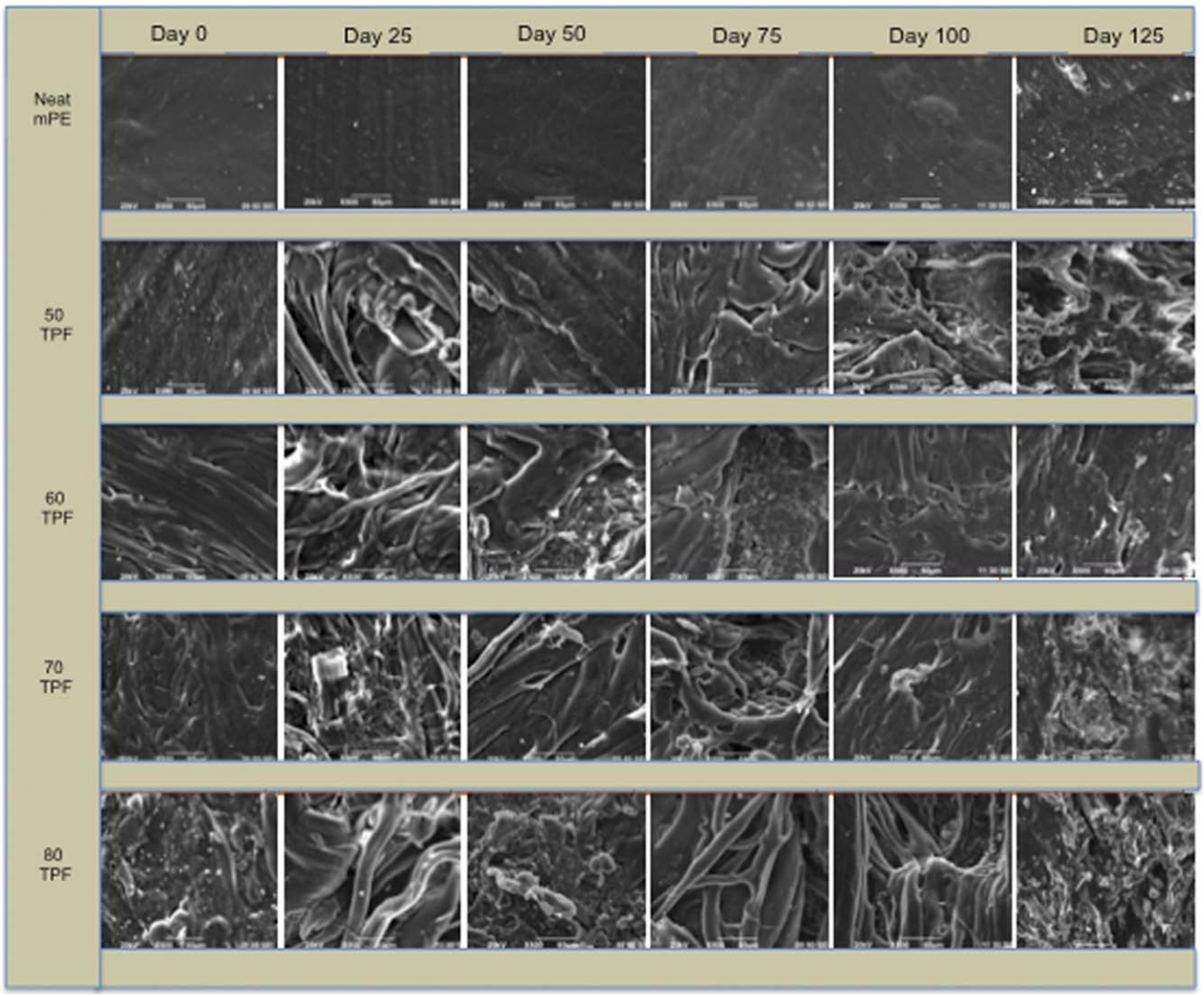

FIG. 10. Chronological microstructural analysis by SEM of the samples under compost during 125 days. [Color figure can be viewed in the online issue, which is available at wileyonlinelibrary.com.]

 DOI 10.1002/pen

more evident at day 125. The 60 TPF did not show a smooth surface at day 0. The flux of the injection was very marked, though a compact material was perceived. However, it was obviously different from the neat material. Micrographs taken from 25 to 125 days clearly showed erosion caused by the microorganisms present in the compost. At day 75, a large hole in the surface was observed. This type of spoilage impacts the weight loss. The 70 TPF also presented a compact structure at the beginning, but evidence of deterioration during composting was evident from 25 to 100 days. At day 125, the sample lost its structure. Finally, the 80 TPF did not have a homogeneous surface at the beginning. The high weight loss observed for this blend could be correlated with the 125 day micrograph, which clearly showed a loss of structure and lack of solidity. In addition, fungal conidia were observed in this micrograph, despite the fact that all the samples were washed with deionized water. Fungi are present in the compost, and the spread of the conidia over the surface of the samples could be explained by their high TPF content.

CONCLUSIONS

A plastic material was generated by blending whitened TPF with mPE at differential proportions. Grafting MA on the molecular chain of the synthetic polymer promoted the homogeneity of the blends. The characteristics of the thermoplastic flour made it feasible to blend it with synthetic polymers to produce biodegradable materials. Blends containing up to 80% thermoplastic banana flour were injection molded. One of our plastic blends, the 50 TPF, exhibited mechanical properties similar to those of neat mPE, making this blend suitable for industrial purposes. Chronological analysis of weight loss and microstructure by SEM confirmed the biodegradability of the blends.

ACKNOWLEDGMENT

The authors thank SIP-IPN.

REFERENCES

1. C. Fang-Chyou, L. Sun-Mou, and T. Kai-Tse, *Polym. Test*., **28**, 243 (2009).
2. S. Narpinder, S. Jaspreet, K. Lovedeep, S.S. Navdeep, and S. Balmeet, *Food Chem*., **81**, 219 (2003).
3. A. Ioannis, G.B. Costas, O. Hiromasa, and K. Norioki, *Carbohydr. Polym*., **89**, 36 (1998).
4. A. Ioannis, G.B. Costas, O. Hiromasa, K. Norioki, and P. Eleni, *Carbohydr. Polym*., **33**, 227 (1997).
5. Z. Pingyi, L.W. Roy, N.B. James, and R.H. Bruce, *Carbohydr. Polym*., **59**, 443 (2005).
6. Y. Lv, L. Gan, M. Liu, W. Xiong, Z. Xu, D. Zhu, and D.S. Wright, *J. Power Sources*, **209**, 152 (2012).
7. J. Thebaudin and A.C. Lefebvre, *Trends Food Sci. Technol*., **8**, 41 (1997).
8. A. Nourbakhsh, A. Ashori, and A.K. Tabrizi, *Compos. B*, **56**, 279 (2014).
9. A. Ashori, *J. Compos. Mater*., **47**, 149 (2013).
10. M. Zahedi, T. Tabarsa, A. Ashori, M. Madhoushi and A. Shakeri, *J. Appl. Polym. Sci*., **129**, 1491 (2013).
11. A. Carlmark, E. Larsson, and E. Malmström, *Eur. Polym. J*., **48**, 1646 (2012).
12. J. Marriott, M. Robinson, and S.K. Karikari, *J. Sci. Food Agric*., **32**, 1021 (1981).
13. N.N. Terra, E. Garcia and F.M. Lajolo, *J. Food Sci*., **48**, 1097 (1983).
14. Food and Agriculture Organization of the United Nations, Available at: http://faostat.fao.org/site/609/default.aspx. Accessed on May 15, 2013.
15. Secretaría de Agricultura, Available at: http://www.sagarpa.gob.mx/AGRICULTURA/Paginas/Agricultura.aspx. Accessed on May 25, 2013
16. N. Cordeiro, M. Ornelas, A. Ashori, S. Sheshmani, and H. Norouzi, *Carbohydr. Polym*., **87**, 2367 (2012).
17. H. Vieyra, M.A. Aguilar-Méndez, and E. San Martín-Martínez, *Starch/Staerke*, **63**, 42 (2011).
18. R. Deanin, *Fillers and Reinforcements for Plastics: Advances in Chemistry Series*, American Chemical Society Publications, Washington DC (1974).
19. F.J. Rodriguez-Gonzalez and B.A. Ramsay, *Polymer*, **44**, 1517 (2003).
20. C. Bastioli, *Biodegradability of Polymer-Mechanisms and Evaluation Methods in Handbook of Biodegradable Polymers*, Rapra Technology Limited, Shawbury, Shrewsbury, Shropshire (2005), 1.
21. S.M. Lai, T.M. Don, and Y.C. Huang, *J. Appl. Polym. Sci*., **100**, 2371 (2006).
22. L.L. Böhm, *Angew. Chem. Int*., **42**, 5010 (2003).
23. A. Ammala, S. Batemana, K. Deana, E. Petinakisa, P. Sangwana, and S. Wonga, *Prog. Polym. Sci*., **36**, 1015 (2011).
24. R. Mülhaupt, *Macromol. Chem. Phys*., **204**, 289 (2003).
25. X. Chen, P. Yu, B. Huang, and P. Long, *Polym. Bull*., **68**, 815 (2012).
26. T.J. Shin, B. Lee, B.S. Seong, Y.S. Han, C.H. Lee, H.H. Son, R.S. Stein, and M. Ree, *Polymer*, **51**, 5799 (2010).
27. A. Takeh, J. Worch, and S. Shanbhag, *Macromolecules*, **44**, 3656 (2011).
28. M. Klapper, Y. Jang, and K. Bieber, *Macromol. Symp*., **213**, 131 (2004).
29. E. Garofalo, L. Incarnato, and L. Di Maio, *Polym. Eng. Sci*., **52**, 1968 (2012).
30. T. Yoo, D.H. Kim, and Y. Son, *J. Appl. Polym. Sci*., **126**, E322 (2012).
31. H. Vieyra, M.A. Aguilar-Méndez, and E. San Martín-Martínez, *J. Appl. Polym. Sci*., **127**, 845 (2013).
32. B.C. Trivedi and B.M. Culbertson, *Maleic Anhydride*, Plenum Press, New York (1982).
33. A. Razak, W. Aizan, L. Tin, and A.A. Yussuf, *Mater. Sci. Eng. C*, **29**, 2370 (2009).
34. M.M. Andrade-Mahecha, D.R. Tapia-Blácido, and F.C. Menegalli, *Carbohydr. Polym*., **88**, 449 (2012).
35. E. Garofalo, M.L. Fariello, L. Di Maio, and L. Incarnato, *Eur. Polym. J*., **49**, 80 (2013).
36. *Industrial colour-difference evaluation*, Technical report. Internationale de I'Eclairage Central Bureau, Vienna (1995).
37. A.J. Meléndez-Martínez, I.M. Vicario, and F.J. Heredia, *J. Agric. Food Chem*., **51**, 7266 (2003).

38. W.R. Morrison and B. Laignelet, *J. Cereal Sci*., **1**, 9 (1983).
39. *Colorimetry*, Technical report. 3rd ed. Commission Internationale de I'Eclairage Central Bureau, Vienna (2004).
40. P.B. Zamudio-Flores, A. Vargas-Torres, F. Gutiérrez-Meraz, and L.A. Bello-Pérez, *Agrociencia*, **44**, 283 (2010).
41. R.L. Whistler, J.N. BeMiller and E.F. Paschall, *Starch, Chemistry and Technology*, 2nd ed., Academic Press, Orlando (1984).
42. K. Kayisu, L.F. Hood, and P.J. Vansoest, *J. Food Sci*., **46**, 1885 (1981).
43. J.G. Jeroen, C. Remko, and D. De Wi, *Ind Crop Prod*., **5**, 1 (1996).
44. M.C. Van der Burgt, M.E. Van der Woude, and L.P.B. Janssen, *J. Vinyl Addit. Technol*., **2**, 170 (1996).
45. P.L. Russel and G. Oliver, *J. Cereal Sci*., **10**, 123 (1989).
46. D. Coral, P. Pineda-Gómez, A. Rosales-Rivera, and M. Rodriguez-García, *J. Phys.: Conf. Ser*., **167**, 1 (2009).
47. P. Zhang and B. Hamaker, *Carbohydr. Polym*., **87**, 1552 (2012).
48. Y. Nishio, T. Haratani, and T. Takahashi, *Macromolecules*, **22**, 2547 (1989).
49. S. Fujita and G. Fujiyama, *Starch/Staerke*, **45**, 436 (1993).
50. S. El-Sayed, K.H. Mahmoud, A.A. Fatah, and A. Hassen, *Phys. B*, **406**, 2068 (2011).
51. L. Shu-Ming, J. Ning, M. Ming-Guo, Z. Zhe, L. Qing-Hong and S. Run-Cang, *Carbohydr. Polym*., **86**, 441 (2011).
52. Dow Chemical Company. Available at: http://msdssearch.dow.com/PublishedLiteratureDOWCOM/dh_0259/0901b803802592a8.pdf?filepath=packaging/pdfs/noreg/774-00101.pdf&fromPage=GetDoc. Accessed on June 4, 2011.
53. A.M. Walker, Y. Tao, and J.M. Torkelson, *Polymer*, **48**, 1066 (2007).
54. A.G. Pedroso and D.S. Rosa, *Carbohydr. Polym*., **59**, 1 (2005).
55. K. Svegmark and A.M. Hermansson, *Food Struct*., **12**, 181 (1993).
56. S. Narpinder, S. Jaspreet, K. Lovedeep, S.S. Navdeep, and S.G. Balmeet, *Food Chem*., **81**, 219 (2003).
57. L.A. Bello-Pérez, E. Agama-Acevedo, S.G. Sayago-Ayerdi, E. Moreno-Damián, and D.C. Figueroa, *Starch/Staerke*, **52**, 68 (2000).
58. M.C. Núñez-Santiago, L.A. Bello-Pérez, and A. Tecant, *Carbohydr. Polym*., **56**, 65 (2004).
59. F.M. Pelissari, M.M. Andrade-Mahecha, P.J. Do Amaral, and F.C. Menegall, *Starch/Staerke*, **64**, 382 (2012).
60. M. Pracella, C. Pancrazi, Md. Minhaz-Ul and Aldo D'Alessio, *J Therm Anal Calorim*., **103**, 95 (2011).
61. National Institute of Advanced Industrial Science and Technology. Available at: http://riodb01.ibase.aist.go.jp/sdbs/. Accessed on April 4, 2012.
62. H. Lateef, S. Grimes, P. Kewcharoenwong, and B. Feinberg, *J. Chem. Technol. Biotechnol*., **84**, 1818 (2009).
63. S. Goheen and R. Wool, *J. Appl. Polym. Sci*., **42**, 2691 (1991).
64. D.M. Suflet, G.C. Chitanu, and V.I. Popa, *React. Funct. Polym*., **66**, 1240 (2006).
65. T. Koichiro, U. Yuichi, and N. Keiji, *Polym. Degrad. Stab*., **98**, 1847 (2013).
66. K. Johnson, A. Pometto, and Z. Nikolov, *Appl. Environ. Microbiol*., **59**, 1155 (1993).
67. Md. Minhaz-Ul, V. Alvarez, M. Paci, and M. Pracella, *Compos. A* **42**, 2060 (2011).
68. M. Vikman, S. Karjomaa, A. Kapanen, K. Wallenius, and M. Itävaara, *Appl. Microbiol. Biotechnol*., **59**, 591 (2002).
69. D.H. Jenings and G. Lysek, *Fungal Biology: Understanding the Fungal Lifestyle*, BIOS Scientific publisher, Oxford (1996).
70. L. Albinas, L. Loreta, and P. Dalia, *Int. Biodeter. Biodegr*., **52**, 233 (2003).

 DOI 10.1002/pen